Nat Hazards (2015) 78:2121–2142
DOI 10.1007/s11069-015-1823-6

ORIGINAL PAPER

Lateral thermal disturbance of embankments in the permafrost regions of the Qinghai-Tibet Engineering Corridor

Mingyi Zhang[1] · Wansheng Pei[1] · Xiyin Zhang[1] · Jianguo Lu[1]

Received: 15 April 2015 / Accepted: 21 May 2015 / Published online: 10 July 2015

Abstract Numerous engineering projects have been completed on the Qinghai-Tibet Plateau, and with continued economic growth, additional important engineering projects are being planned. Major transportation construction is largely restricted to the Qinghai-Tibet Engineering Corridor, which is as narrow as a few hundred meters in some places. In this narrow corridor, projects such as the Qinghai-Tibet Railway and the Qinghai-Tibet Highway can influence the stability of the permafrost. We use a numerical model to investigate the individual thermal disturbance caused by the Qinghai-Tibet Railway, the Qinghai-Tibet Highway, and the planned Qinghai-Tibet Expressway. To simulate an upper limit of disturbance under current climate we use the most unfavorable combination of engineering design practices, with unprotected embankments, a traditional ballast embankment for the Qinghai-Tibet Railway, and traditional asphalt pavement embankments for the Qinghai-Tibet Highway and the Qinghai-Tibet Expressway. The lateral thermal disturbance extent of the three projects increases linearly with embankment height. Under the same embankment heights, the lateral extent of thermal disturbance is smallest for the Qinghai-Tibet Railway and is largest for the full Qinghai-Tibet Expressway. The model results provide guidance for minimum distances between the transportation projects to prevent thermal interaction, as a function of embankment height and design. In future research it is important to evaluate the thermal disturbance scopes of other engineering structures, such as tunnels, bridges, and oil pipelines, and to evaluate the thermal interaction and cumulative impact of multiple structures under current and future climate scenarios.

Keywords Lateral thermal disturbance · Embankment · Permafrost region · Qinghai-Tibet Engineering Corridor

✉ Mingyi Zhang
myzhang@lzb.ac.cn

[1] State Key Laboratory of Frozen Soil Engineering, Cold and Arid Regions Environmental and Engineering Research Institute, Chinese Academy of Sciences, Lanzhou 730000, China

1 Introduction

The Qinghai-Tibet Plateau has a permafrost area of about 1.5×10^6 km^2 (Zhou et al. 2000), and this permafrost is sensitive to thermal disturbance that can result from engineering infrastructure projects. Numerous engineering projects have been completed on the Qinghai-Tibet Plateau, and with continued economic growth, additional major engineering infrastructure projects are being planned. These major projects are restricted to a narrow zone, the *Qinghai-Tibet Engineering Corridor*, to minimize the disturbance to the surrounding environments and to facilitate the construction and maintenance (Jin et al. 2008; Ma et al. 2012). The Qinghai-Tibet Engineering Corridor crosses many areas of relatively warm permafrost and is as narrow as a few hundred meters in some places (Cheng 2002; Jin et al. 2008; Ma et al. 2012). The engineering projects such as the Qinghai-Tibet Railway and the Qinghai-Tibet Highway (Fig. 1) can affect the stability of the permafrost and interact thermally in this narrow zone (Jin et al. 2008; Ma et al. 2012).

Engineering projects can change the original ground surface conditions in permafrost regions, causing degradation of the permafrost and the associated ecological environment (Wu et al. 1988, 2003; Jin et al. 2008; Lai et al. 2009a; Peng et al. 2015). Thermal interactions between projects will also affect the stability of each project if their locations are too close in permafrost regions (Ma et al. 2012). In China, about 630 km of the length of the Qinghai-Tibet Highway passes through permafrost regions (Wang et al. 2004), and in 1990 about 346 km had experienced thaw settlement, frost heaving and frost boiling (Wu and Tong 1995). Similarly 632 km of the length of the Qinghai-Tibet Railway from Golmud to Lhasa, completed in 2006, goes through permafrost regions, and there are concerns that freezing-thawing hazards might potentially influence roadbed stability (Niu et al. 2011). In a permafrost setting in Russia a 1994 survey showed that the damage ratio was 27.5 % for the Baikal–Amur Mainline (BAM) Railway (Cheng 2005), which provides some indication of the potential scale of future damage for the Qinghai-Tibet Railway.

The previous work mentioned above has investigated these engineering projects individually; however, there has been no quantitative evaluation of the potential thermal interaction between these engineering projects that could guide design decisions and planning. Quantitative evaluation is a key way to address this question and ensure the long-term survival of both the permafrost environment and engineering projects in the Qinghai-

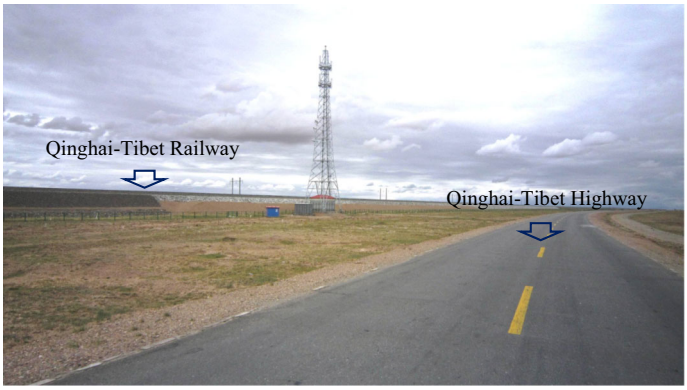

Fig. 1 Example of transportation infrastructure in the Qinghai-Tibet Engineering Corridor

Tibet Engineering Corridor. The Qinghai-Tibet Expressway is currently being planned, and an important design question is how far the new structure should be away from the existing Qinghai-Tibet Railway and Qinghai-Tibet Highway to avoid thermal interactions.

Therefore in the work reported here we evaluate the potential thermal interaction of railway and highway projects in the Qinghai-Tibet Engineering Corridor by quantifying the thermal disturbance scopes of different embankment types. A numerical model is used to investigate the thermal disturbance scopes for the three major engineering projects in the engineering corridor: the Qinghai-Tibet Railway, the Qinghai-Tibet Highway, and the Qinghai-Tibet Expressway. For conservative engineering design we examine the most unfavorable combination of engineering design practices, with unprotected embankment construction for the three projects. Model results provide information on the lateral extent of thermal disturbance for each project, which can be used to evaluate potential thermal interaction between the existing Qinghai-Tibet Railway and Qinghai-Tibet Highway in the narrow Qinghai-Tibet Engineering Corridor, and can be used in the planned Qinghai-Tibet Expressway.

2 Model description

2.1 Computational domains

In this study we select a traditional ballast embankment for the Qinghai-Tibet Railway and traditional asphalt pavement embankments for the Qinghai-Tibet Highway and the Qinghai-Tibet Expressway. The computational domains for the three embankment types are shown in Figs. 2, 3, and 4. They are based on the Temporary Code for Engineering Construction of Railway in Permafrost Regions of the Qinghai-Tibet Plateau (2003), on the Design Specifications for Highway Alignment (2006), on the related references (Lai et al. 2009a; Chen et al. 2012), and on the practical embankment geometries at an elevation of about 4500 m in the Qinghai-Tibet Engineering Corridor. The computational domains are all extended 100 m outwards from the side-slope toes (A and F) of the embankments, and 50 m downwards from the natural ground surfaces (LA and FG). Other geometries of the computational domains are described below.

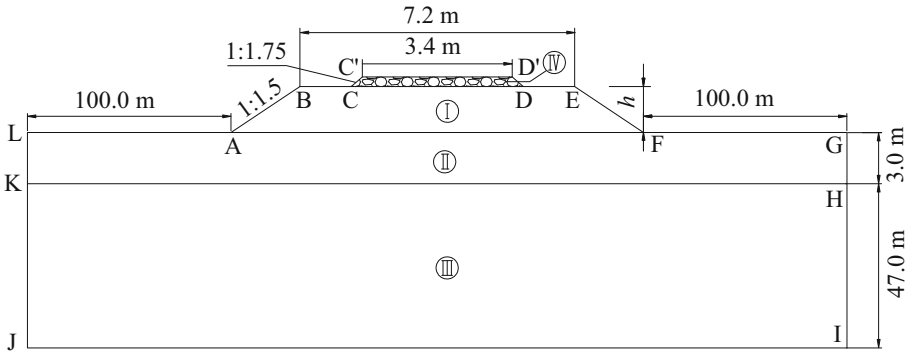

Fig. 2 Computational domain of the traditional ballast embankment for the Qinghai-Tibet Railway. I embankment fill layer, II silty clay layer, III strongly weathered mudstone layer, IV railway ballast layer

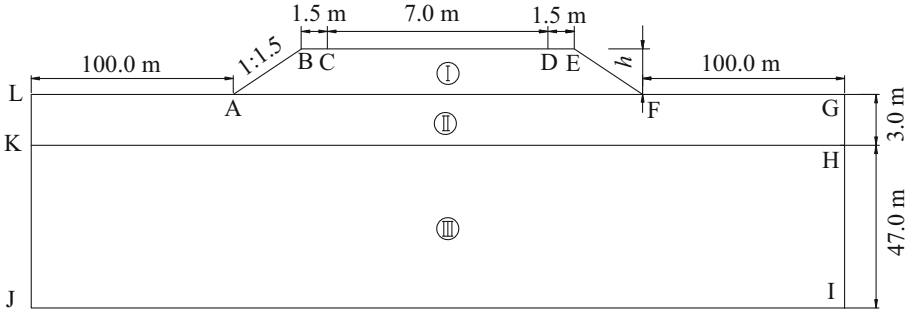

Fig. 3 Computational domain of the traditional asphalt pavement embankment for the Qinghai-Tibet Highway. I embankment fill layer, II silty clay layer, III strongly weathered mudstone layer

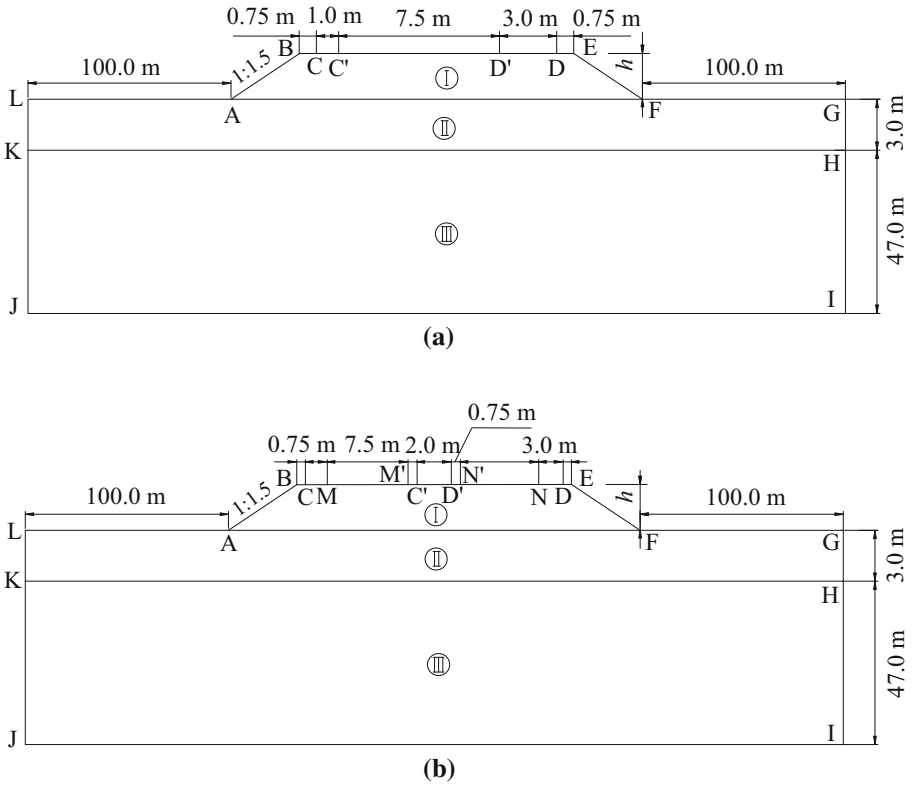

Fig. 4 Computational domain of the traditional asphalt pavement embankment for the Qinghai-Tibet Expressway. I embankment fill layer, II silty clay layer, III strongly weathered mudstone layer. **a** Separated expressway embankment. **b** Full expressway embankment

The computational domain of the traditional ballast embankment for the Qinghai-Tibet Railway is shown in Fig. 2. The top width of the embankment is 7.2 m. The boundaries ABC and DEF are the embankment fill layer surfaces, and the boundary CC′D′D is the railway ballast layer surface.

The computational domain of the traditional asphalt pavement embankment for the Qinghai-Tibet Highway is shown in Fig. 3. The top width of the embankment is 10.0 m. The boundaries ABC and DEF are the embankment fill layer surfaces, and the boundary CD is the asphalt pavement surface.

The computational domains of the traditional asphalt pavement embankments for the Qinghai-Tibet Expressway are shown in Fig. 4a, b. The top width of the full expressway embankment (Fig. 4b) is usually about 26 m. When the roadway crosses the area with complex topography or with sensitive permafrost underlain, the construction of the Qinghai-Tibet Expressway may prefer to using a wide, open land to separate opposing traffic flows rather than using a median strip. Using this construction method, a separated embankment (Fig. 4a) only needs a top width of about 13 m. For this separated embankment (Fig. 4a), the boundaries ABC and DEF are the embankment fill layer surfaces and the boundary CC′D′D is the asphalt pavement surface. For the full embankment (Fig. 4b), the boundaries ABC and DEF are the embankment fill layer surfaces, the boundaries CMM′C′ and D′N′ND are the asphalt pavement surfaces, and the boundary C′D′ is the median strip with embankment fill layer surface.

2.2 Governing equations

In the models the railway ballast layer is treated as a porous media because of its high permeability. The soil layers are treated as solid media, and convection can be neglected in the soil layers because the heat conduction is far larger than the convection (more than 100–1000 times) (An 1990). The governing equations of heat transfer in the two kinds of media are described as follows.

2.2.1 Railway ballast layer

The thermal convection of air inside the railway ballast layer involves heat and mass transfer. In these conditions the air convection is unsteady, and in this analysis only the motion of interstitial air is considered. Therefore the governing equations for mass, momentum, energy can be written as follows (Nield and Bejan 1992; Kong and Wu 2002; Lai et al. 2009a):

Continuity:

$$\frac{\partial v_x}{\partial x} + \frac{\partial v_y}{\partial y} = 0 \tag{1}$$

where v_x and v_y are the x and y components of air velocities, respectively.

Momentum:

$$\frac{\partial p}{\partial x} = -\frac{\mu}{k} v_x - \rho_a B|v| v_x \tag{2a}$$

$$\frac{\partial p}{\partial y} = -\frac{\mu}{k} v_y - \rho_a B|v| v_y - \rho_a^* g \tag{2b}$$

where $|v| = \sqrt{v_x^2 + v_y^2}$, B is the *Beta* factor of non-Darcy flow, k is the permeability of porous media, μ is the dynamic viscosity of air, p is air pressure, ρ_a is the air density and $\rho_a B|v| v_x$ is the inertia–turbulent term.

It is assumed that the air in the model is incompressible, and its density is only a function of temperature so that the Boussinesq approximation (Kong 1999; Nield and Bejan 1992) can be employed to simplify the analysis.

$$\rho_a^* = \rho_a[1 - \beta(T - T_0)] \tag{3}$$

where T and T_0 are the corresponding temperatures of air density ρ_a^* and ρ_a, respectively, and β is the coefficient of thermal expansion for air.

Energy:

$$C_e^* \frac{\partial T}{\partial t} = \frac{\partial}{\partial x}\left(\lambda_e^* \frac{\partial T}{\partial x}\right) + \frac{\partial}{\partial y}\left(\lambda_e^* \frac{\partial T}{\partial y}\right) - c_a \rho_a \left(v_x \frac{\partial T}{\partial x} + v_y \frac{\partial T}{\partial y}\right) \tag{4}$$

where c_a is the specific heat of air at a constant pressure and C_e^* and λ_e^* are the effective volumetric heat capacity and effective thermal conductivity of porous media, respectively.

2.2.2 Soil layers

Because convection can be neglected in the soil layer, only heat conduction and phase change are considered and so the heat transfer process can be described as (Bonacina et al. 1973; An 1990; Zhao 2002):

$$C_e^* \frac{\partial T}{\partial t} = \frac{\partial}{\partial x}\left(\lambda_e^* \frac{\partial T}{\partial x}\right) + \frac{\partial}{\partial y}\left(\lambda_e^* \frac{\partial T}{\partial y}\right) \tag{5}$$

It is assumed that the phase change occurs in a temperature range of $T_m \pm \Delta T$. When the effective heat capacity is constructed, the effect of a temperature interval $2\Delta T$ is included. Assuming that C_f, C_u, λ_f, and λ_u do not depend on temperature, the following expressions for C_e^* and λ_e^* are obtained (Bonacina et al. 1973; Guo et al. 1999):

$$C_e^* = \begin{cases} C_f & T < T_m - \Delta T \\ \dfrac{L}{2\Delta T} + \dfrac{C_f + C_u}{2} & T_m - \Delta T \le T \le T_m + \Delta T \\ C_u & T > T_m + \Delta T \end{cases} \tag{6a}$$

$$\lambda_e^* = \begin{cases} \lambda_f & T < T_m - \Delta T \\ \lambda_f + \dfrac{\lambda_u - \lambda_f}{2\Delta T}[T - (T_m - \Delta T)] & T_m - \Delta T \le T \le T_m + \Delta T \\ \lambda_u & T > T_m + \Delta T \end{cases} \tag{6b}$$

where subscripts f and u represent the frozen and unfrozen states, respectively; C_f and λ_f are the volumetric heat capacity and thermal conductivity of media in the frozen area, respectively; C_u and λ_u are the volumetric heat capacity and thermal conductivity of media in the unfrozen area, respectively; and L is the latent heat per unit volume.

2.3 Boundary and initial conditions

The upper boundary conditions for embankments are controlled by a range of factors, e.g., solar radiation, air convection, evaporation, and so on. To simplify the boundary conditions in the models, temperatures are applied to the upper boundaries. The present mean annual air temperature is taken as −4.0 °C, and based on adherent layer theory (Zhu 1988) and the related reference (Lai et al. 2009a), the temperature boundary conditions are given as follows:

Temperatures for natural ground surfaces (boundaries LA and FG, Figs. 2, 3, 4):

$$T_{\text{nature}} = -1.5 + 12\sin\left(\frac{2\pi}{8760}t_{\text{h}} + \frac{\pi}{2} + \alpha_0\right) \tag{7}$$

Temperatures at the side-slope and embankment fill layer surfaces (boundaries ABC and DEF, Figs. 2, 3, 4; boundaries CC′ and D′D, Fig. 2; boundary C′D′, Fig. 4b):

$$T_{\text{slope}} = 0.7 + 13\sin\left(\frac{2\pi}{8760}t_{\text{h}} + \frac{\pi}{2} + \alpha_0\right) \tag{8}$$

Temperature at the top surface of the railway ballast layer (boundary C′D′, Fig. 2):

$$T_{\text{ballast top}} = 1.5 + 15\sin\left(\frac{2\pi}{8760}t_{\text{h}} + \frac{\pi}{2} + \alpha_0\right) \tag{9}$$

Temperatures at the asphalt pavement surfaces (boundary CD, Fig. 3; boundary CC′D′D, Fig. 4a; boundaries CMM′C′ and D′N′ND, Fig. 4b):

$$T_{\text{asphalt top}} = 2.5 + 15\sin\left(\frac{2\pi}{8760}t_{\text{h}} + \frac{\pi}{2} + \alpha_0\right) \tag{10}$$

where t_{h} is time and α_0 is a phase angle determined by the finishing time of the embankment. Where two boundaries meet, the temperature is given by the mean value of the two boundary conditions.

In the three models the geothermal heat flux at the bottom boundary (JI, Figs. 2, 3, 4) is a constant of 0.06 W/m^2 and the lateral boundaries (LKJ and GHI, Figs. 2, 3, 4) are assumed to be adiabatic (Lai et al. 2003, 2009a).

It is assumed that the embankments are constructed on July 15. The initial temperature fields of the natural soil layers (Parts II and III, Figs. 2, 3, 4) are obtained through a long-term transient solution with the upper boundary condition (Eq. 7). The temperatures of the railway ballast and embankment fill layers are taken as the shallow ground temperature on July 15.

3 Results and analysis

In this study the temperature distributions for all cases are simulated for a total of 50 years and the lateral thermal disturbance is evaluated from output for July 15 each year based on the construction date (July 15). The mean annual ground temperature is usually taken as the temperature at the depth of 0.1 °C annual amplitude of ground temperature because of the limit of test precision (Qin et al. 2014); therefore, considering the requirement of

Table 1 Physical parameters of the media in the models (Lai et al. 2003, 2009a)

Soil type	λ_{f} W/(m °C)	C_{f} J/(m^3 °C)	λ_{u} W/(m °C)	C_{u} J/(m^3 °C)	L J/m^3
Railway ballast layer	0.346	1.006×10^6	0.346	1.006×10^6	0.0
Embankment fill layer	1.980	1.913×10^6	1.919	2.227×10^6	2.04×10^7
Silty clay layer	1.351	1.879×10^6	1.125	2.357×10^6	6.03×10^7
Strongly weathered mudstone layer	1.824	1.846×10^6	1.474	2.099×10^6	3.77×10^7

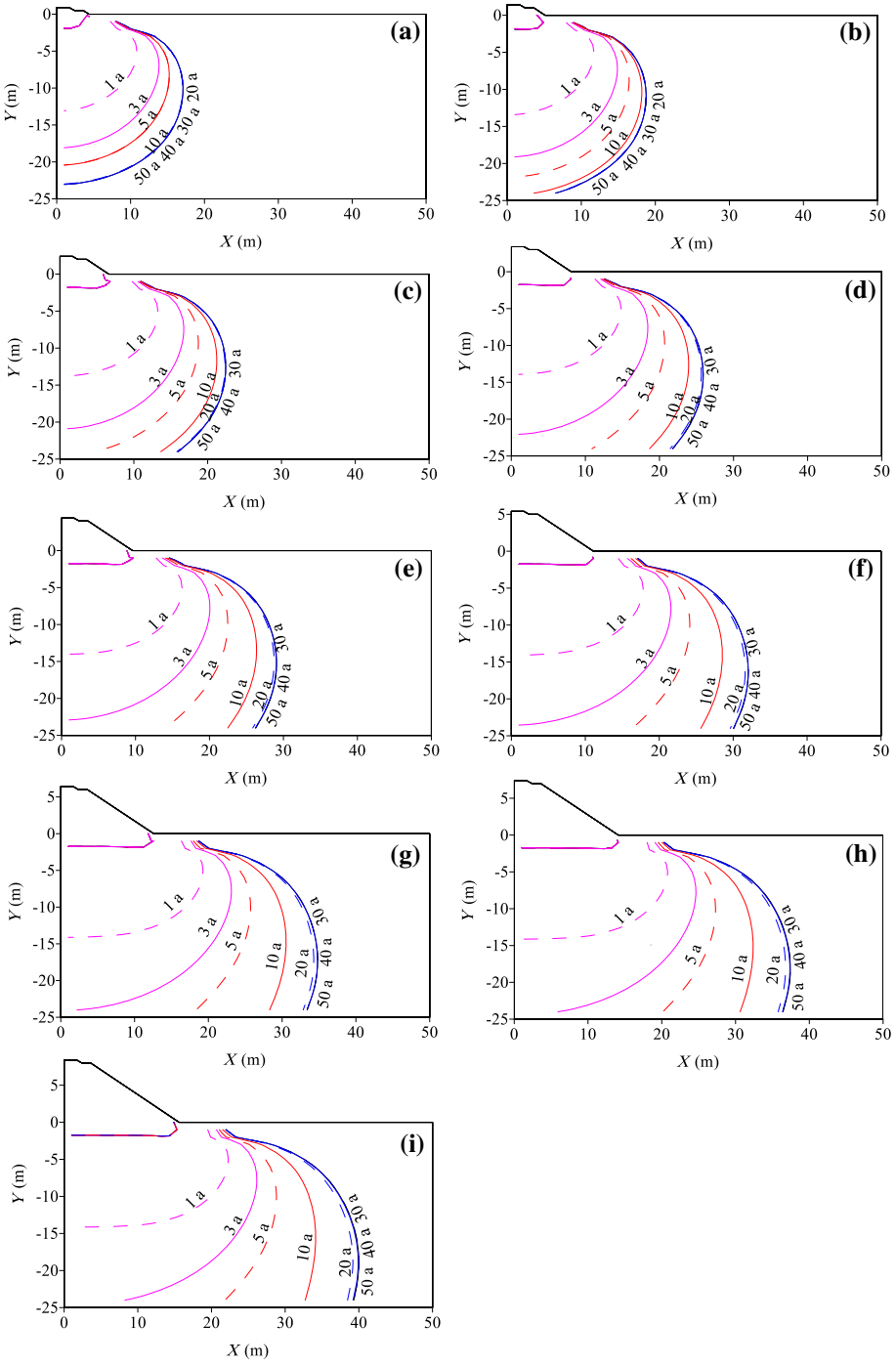

Fig. 5 Isolines for ground temperature change of 0.1 °C under different embankment heights for the Qinghai-Tibet Railway. **a** 0.5 m, **b** 1.0 m, **c** 2.0 m, **d** 3.0 m, **e** 4.0 m, **f** 5.0 m, **g** 6.0 m, **h** 7.0 m, and **i** 8.0 m. Isolines are labeled in years (**a**) after construction, and *X* is distance and *Y* is depth

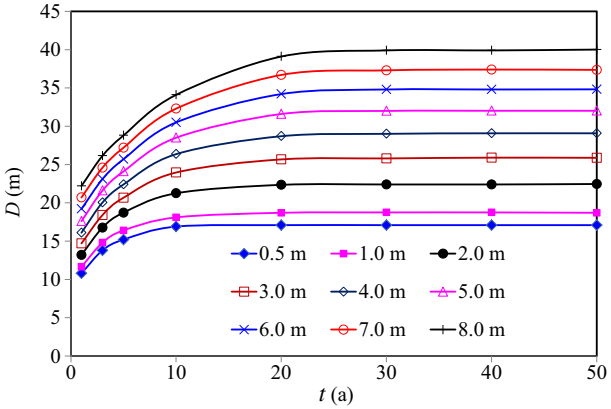

Fig. 6 Temporal changes in the lateral thermal disturbance distance for different embankment heights for the Qinghai-Tibet Railway

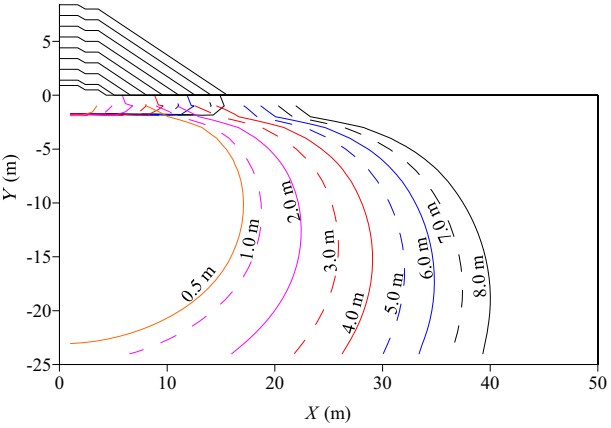

Fig. 7 Thermal disturbance extent for different embankment heights in the 50th year after construction for the Qinghai-Tibet Railway

Table 2 Lateral thermal disturbance distance for different embankment heights for the Qinghai-Tibet Railway

Embankment height (m)	Lateral thermal disturbance distance (m)
0.5	17.09
1.0	18.70
2.0	22.46
3.0	25.88
4.0	29.08
5.0	32.02
6.0	34.82
7.0	37.36
8.0	40.01

engineering practices, we define thermal disturbance as a change in ground temperature of 0.1 °C or more compared to conditions without the embankment. Thus the isoline for a ground temperature change of 0.1 °C is regarded as the limit of the thermal disturbance caused by the embankment. We take the maximum distance between the embankment

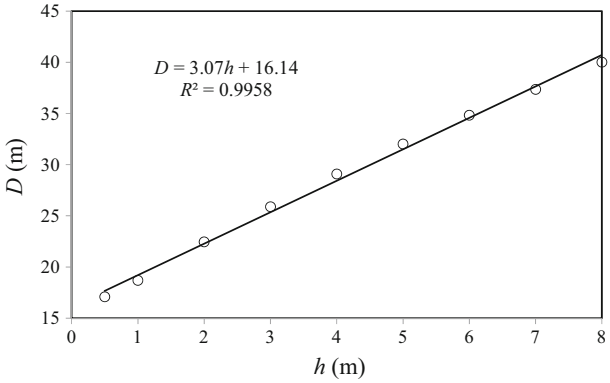

Fig. 8 Relationship between lateral thermal disturbance distance and embankment height for the Qinghai-Tibet Railway

centerline and the 0.1 °C ground temperature change isoline in the 50th year after construction as the lateral thermal disturbance distance of the embankment.

3.1 Qinghai-Tibet Railway embankment

In the traditional ballast embankment model for the Qinghai-Tibet Railway (Fig. 2) nine embankment heights are selected to cover the range of actual embankment heights: 0.5, 1.0, 2.0, 3.0, 4.0, 5.0, 6.0, 7.0, and 8.0 m.

In the model the permeability and inertial resistance factor (*Beta* factor of non-Darcy flow) of the railway ballast layer are $k = 2.34 \times 10^{-6}$ m^2 and $B = 90.55$ m^{-1}, respectively (Zhang et al. 2009). The physical parameters of air at an elevation of about 4500 m (Lai et al. 2003, 2009a): the specific heat is $c_a = 1.004 \times 10^3$ J/(kg °C), the thermal conductivity is $\lambda = 2.0 \times 10^{-2}$ W/(m °C), the air density is $\rho_a = 0.641$ kg/m^3, and the dynamic viscosity is $\mu = 1.75 \times 10^{-5}$ kg/(m s). The other physical parameters of the media are listed in Table 1.

The lateral thermal disturbance extent for the railway embankment expands quickly to a relatively steady state (Figs. 5, 6). The 0.5-m embankment reaches a steady state in about 10 years, and the 8-m embankment takes more than 20 years to reach a steady state. In all cases there is no obvious expansion of the thermal disturbance after 30 years. The extent of thermal disturbance for different embankment heights in the 50th year after construction for the Qinghai-Tibet Railway is shown in Fig. 7. Based on Fig. 7, the lateral thermal disturbance distances of embankment under different embankment heights are listed in Table 2. The lateral extent of the thermal disturbance at steady state increases linearly ($R^2 = 0.9958$) with embankment height (Table 2; Fig. 8), indicating that embankment height is a key factor in determining the lateral thermal disturbance distance of an embankment for the Qinghai-Tibet Railway.

3.2 Qinghai-Tibet Highway embankment

In the traditional asphalt pavement embankment model for the Qinghai-Tibet Highway (Fig. 3) nine embankment heights are selected to cover the range of actual embankment heights: 0.5, 1.0, 2.0, 3.0, 4.0, 5.0, 6.0, 7.0, and 8.0 m. The physical parameters of media are listed in Table 1.

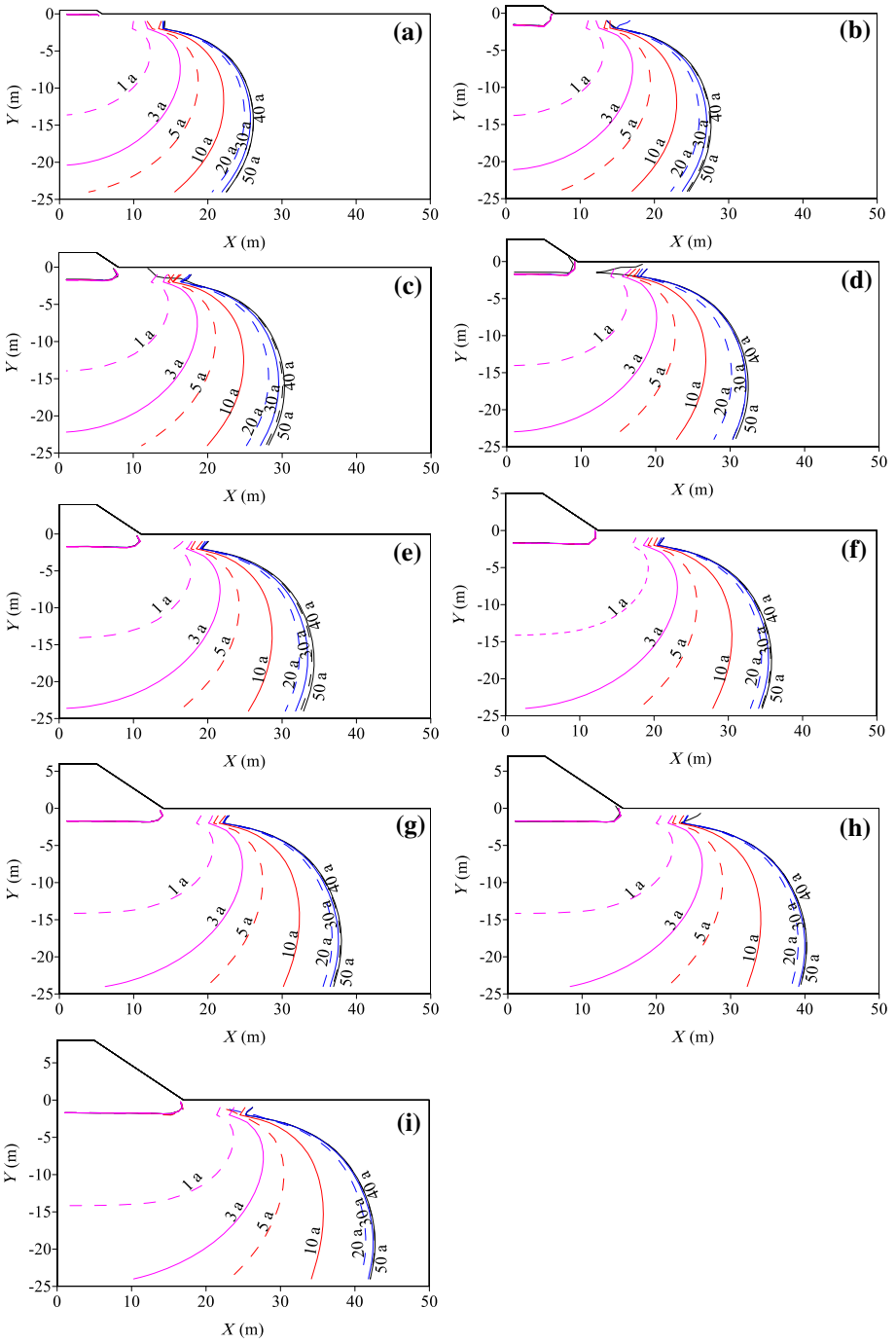

Fig. 9 Isolines for ground temperature change of 0.1 °C under different embankment heights for the Qinghai-Tibet Highway. **a** 0.5 m, **b** 1.0 m, **c** 2.0 m, **d** 3.0 m, **e** 4.0 m, **f** 5.0 m, **g** 6.0 m, **h** 7.0 m, and **i** 8.0 m. Isolines are labeled in years (**a**) after construction, and *X* is distance and *Y* is depth

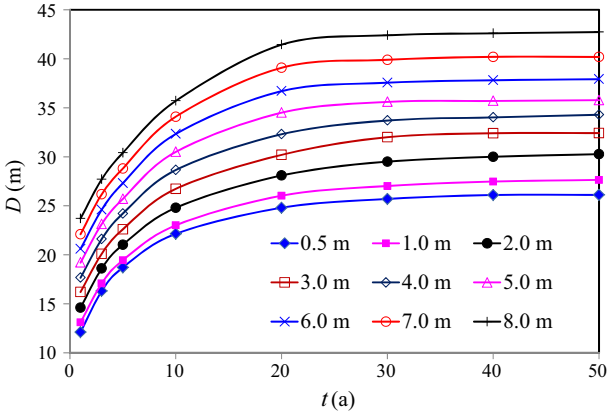

Fig. 10 Temporal changes in the lateral thermal disturbance distance for different embankment heights for the Qinghai-Tibet Highway

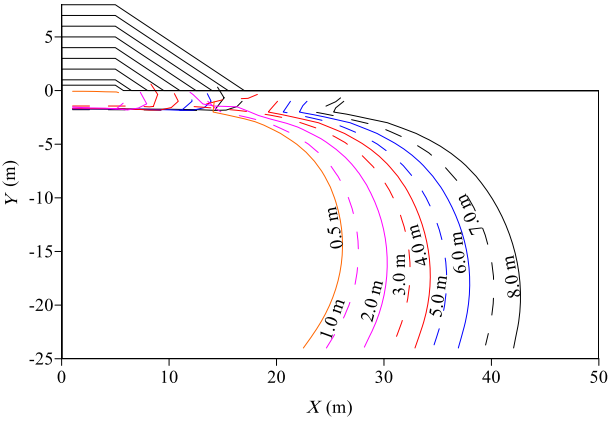

Fig. 11 Thermal disturbance extent for different embankment heights in the 50th year after construction for the Qinghai-Tibet Highway

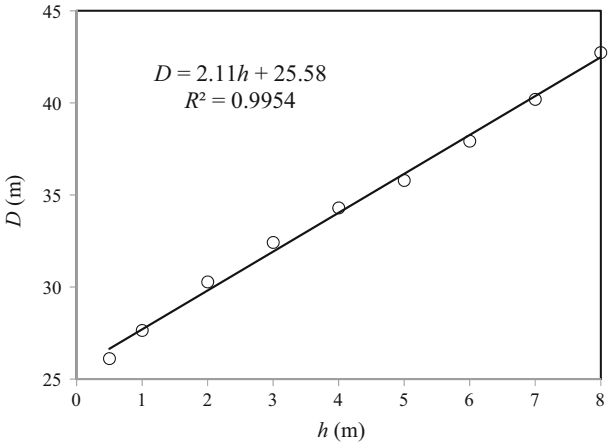

Fig. 12 Relationship between lateral thermal disturbance distance and embankment height for the Qinghai-Tibet Highway

Table 3 Lateral thermal disturbance distance for different embankment heights for the Qinghai-Tibet Highway

Embankment height (m)	Lateral thermal disturbance distance (m)
0.5	26.11
1.0	27.64
2.0	30.27
3.0	32.42
4.0	34.29
5.0	35.78
6.0	37.92
7.0	40.19
8.0	42.73

The lateral thermal disturbance extent for the Qinghai-Tibet Highway embankment expands quickly with time in previous 30 years and then reach to a relatively steady state (Figs. 9, 10). In all cases there is no obvious expansion of the thermal disturbance after 40 years (Figs. 9, 10). Similarly the lateral extent of the thermal disturbance at steady state increases linearly ($R^2 = 0.9954$) with embankment height (Figs. 11, 12; Table 3), indicating that embankment height is a key factor in determining the lateral thermal disturbance distance of an embankment for the Qinghai-Tibet Highway.

3.3 Qinghai-Tibet Expressway embankment

In the traditional asphalt pavement embankment model for the Qinghai-Tibet Expressway (Fig. 4a, b) nine embankment heights are selected: 0.5, 1.0, 2.0, 3.0, 4.0, 5.0, 6.0, 7.0, and 8.0 m for the separated embankment (Fig. 4a) and the full embankment (Fig. 4b), respectively. The physical parameters of the media are listed in Table 1.

3.3.1 Separated embankment

The lateral thermal disturbance for the separated Qinghai-Tibet Expressway embankment reaches a steady state in about 40 years (Figs. 13, 14). The lateral extent of the thermal disturbance after 50 years of construction increases linearly ($R^2 = 0.9964$) with embankment height (Figs. 15, 16; Table 4), indicating that embankment height is again a key factor in determining the lateral thermal disturbance distance for the separated Qinghai-Tibet Expressway embankment.

3.3.2 Full embankment

The lateral thermal disturbance extent for the full Qinghai-Tibet Expressway embankment does not reach a steady state in 50 years of simulation, but has a relatively slow expansion after 30 years of construction (Fig. 17, 18) because of the more heat input caused by the wide and high-temperature asphalt pavement. The lateral extent of the thermal disturbance in the 50th year after construction increases linearly ($R^2 = 0.9949$) with embankment height (Figs. 19, 20; Table 5), indicating that embankment height is again a key factor in determining the lateral thermal disturbance distance for the full Qinghai-Tibet Expressway embankment.

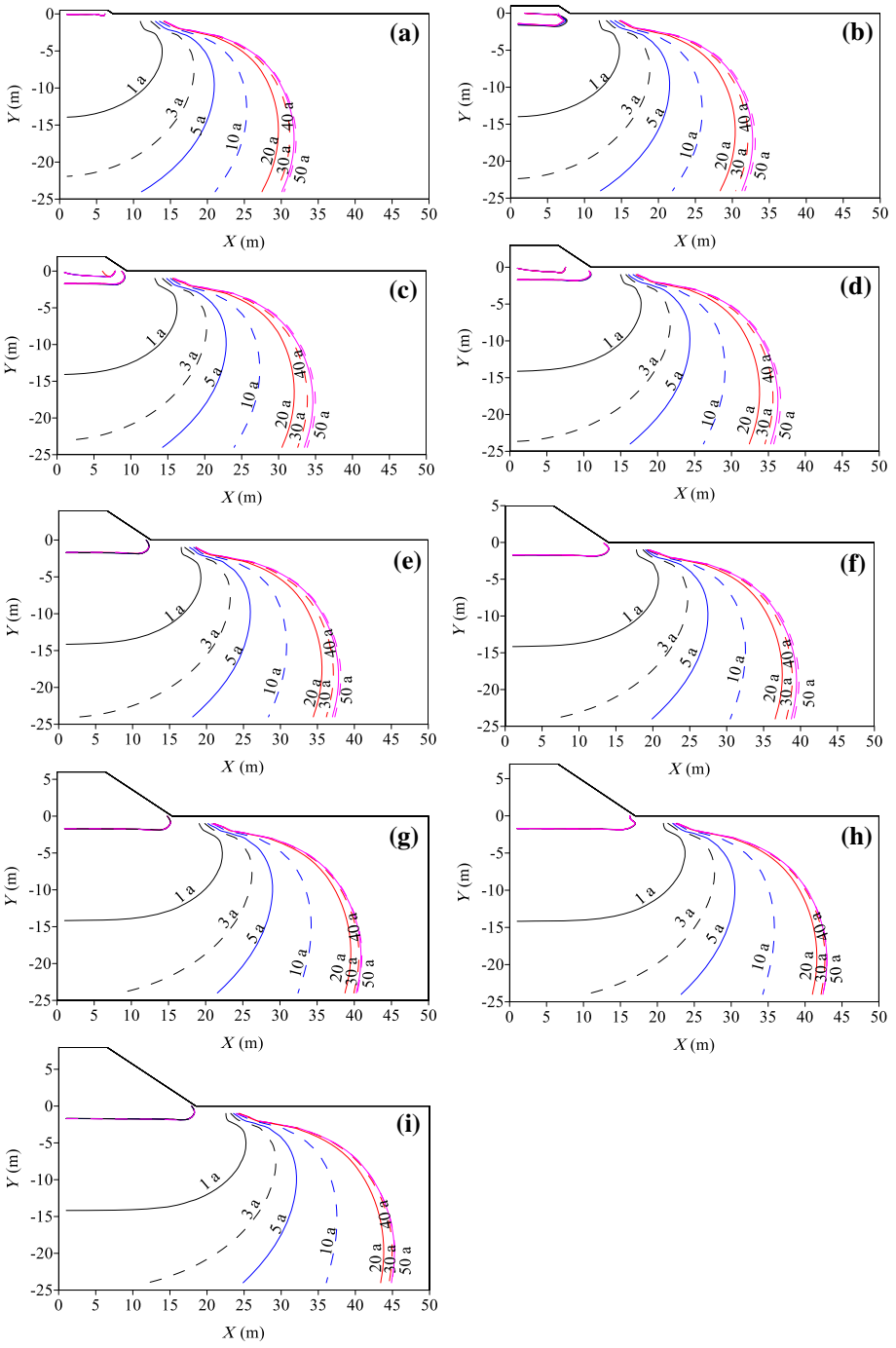

Fig. 13 Isolines for ground temperature change of 0.1 °C under different embankment heights for the separated Qinghai-Tibet Expressway. **a** 0.5 m, **b** 1.0 m, **c** 2.0 m, **d** 3.0 m, **e** 4.0 m, **f** 5.0 m, **g** 6.0 m, **h** 7.0 m, and **i** 8.0 m. Isolines are labeled in years (**a**) after construction, and *X* is distance and *Y* is depth

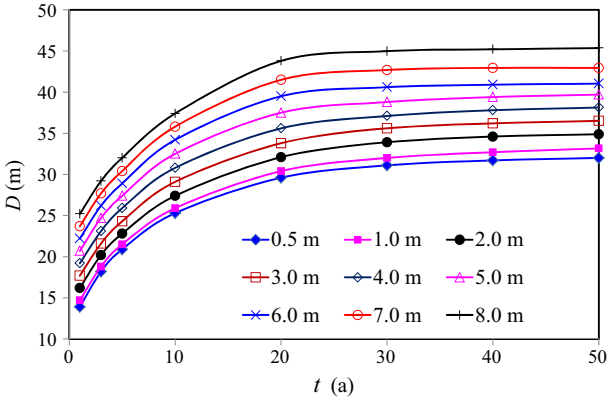

Fig. 14 Temporal changes in the lateral thermal disturbance distance for different embankment heights for the separated Qinghai-Tibet Expressway

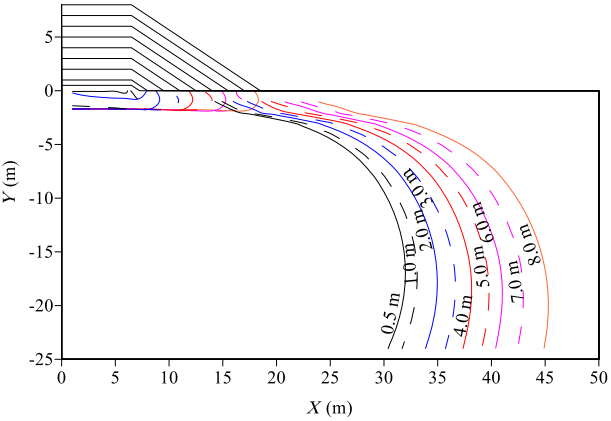

Fig. 15 Thermal disturbance extent for different embankment heights in the 50th year after construction for the separated Qinghai-Tibet Expressway

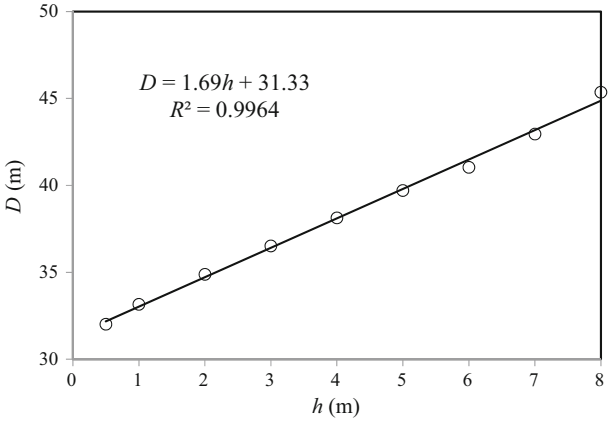

Fig. 16 Relationship between lateral thermal disturbance distance and embankment height for the separated Qinghai-Tibet Expressway

Table 4 Lateral thermal disturbance distance for different embankment heights for the separated Qinghai-Tibet Expressway

Embankment height (m)	Lateral thermal disturbance distance (m)
0.5	32.01
1.0	33.16
2.0	34.88
3.0	36.51
4.0	38.13
5.0	39.70
6.0	41.04
7.0	42.95
8.0	45.36

4 Discussion

The simulation results indicate that embankment height is a key factor in determining the lateral extent of thermal disturbance of each type of embankment (Figs. 8, 12, 16, 20). However, under the same embankment height the lateral extent of thermal disturbance is smallest for the Qinghai-Tibet Railway and largest for the full Qinghai-Tibet Expressway. Furthermore, the slope of the regression equation between lateral thermal disturbance distance and embankment height varies (Table 6) and is largest for the Qinghai-Tibet Railway (3.07) and smallest for the full Qinghai-Tibet Expressway (1.14). This is related to the characteristics of embankment surface. For the Qinghai-Tibet Railway, the top surface of ballast layer is relatively narrow with a relatively lower mean annual temperature (1.5 °C), and side slopes can have a relatively larger effect on the lateral thermal disturbance distance of embankment; therefore, the embankment height has a relatively significant influence to the lateral thermal disturbance distance. However, for the Qinghai-Tibet Highway and the Qinghai-Tibet Expressway, the wider asphalt pavement with a higher mean annual temperature (2.5 °C) results into the fact that the effect of side slopes is relatively weakened. In particular the widest asphalt pavement of the full Qinghai-Tibet Expressway determines its largest lateral thermal disturbance extent under same embankment height. However, if the separated Qinghai-Tibet Expressway with double embankments is considered, its lateral thermal disturbance extent will be larger than that of the full Qinghai-Tibet Expressway.

The lateral thermal disturbance distance for various embankment heights can be calculated from the equations in Table 6 for the railway and each highway type. This allows for a quantitative evaluation of the potential for thermal interaction between the Qinghai-Tibet Railway and the Qinghai-Tibet Highway, as well as calculation of a minimum distance from the existing Qinghai-Tibet Railway and Qinghai-Tibet Highway as a part of the design of the new Qinghai-Tibet Expressway. The results also allow for determination of the minimum width of an engineering corridor as a function of embankment height and embankment type. For example, for the Qinghai-Tibet Railway, the Qinghai-Tibet Highway, and the separated Qinghai-Tibet Expressway (Fig. 21), when their embankment heights are all 8.0 m, based on Table 6, the combined lateral thermal disturbance distance indicates that a minimum of 345.72 m would be required to avoid the lateral thermal disturbance to circumstance and to eliminate their thermal interaction in the Qinghai-Tibet Engineering Corridor. If the full Qinghai-Tibet Expressway is constructed, the minimum distance of the combined lateral thermal disturbance is about 274.28 m. Though the lateral

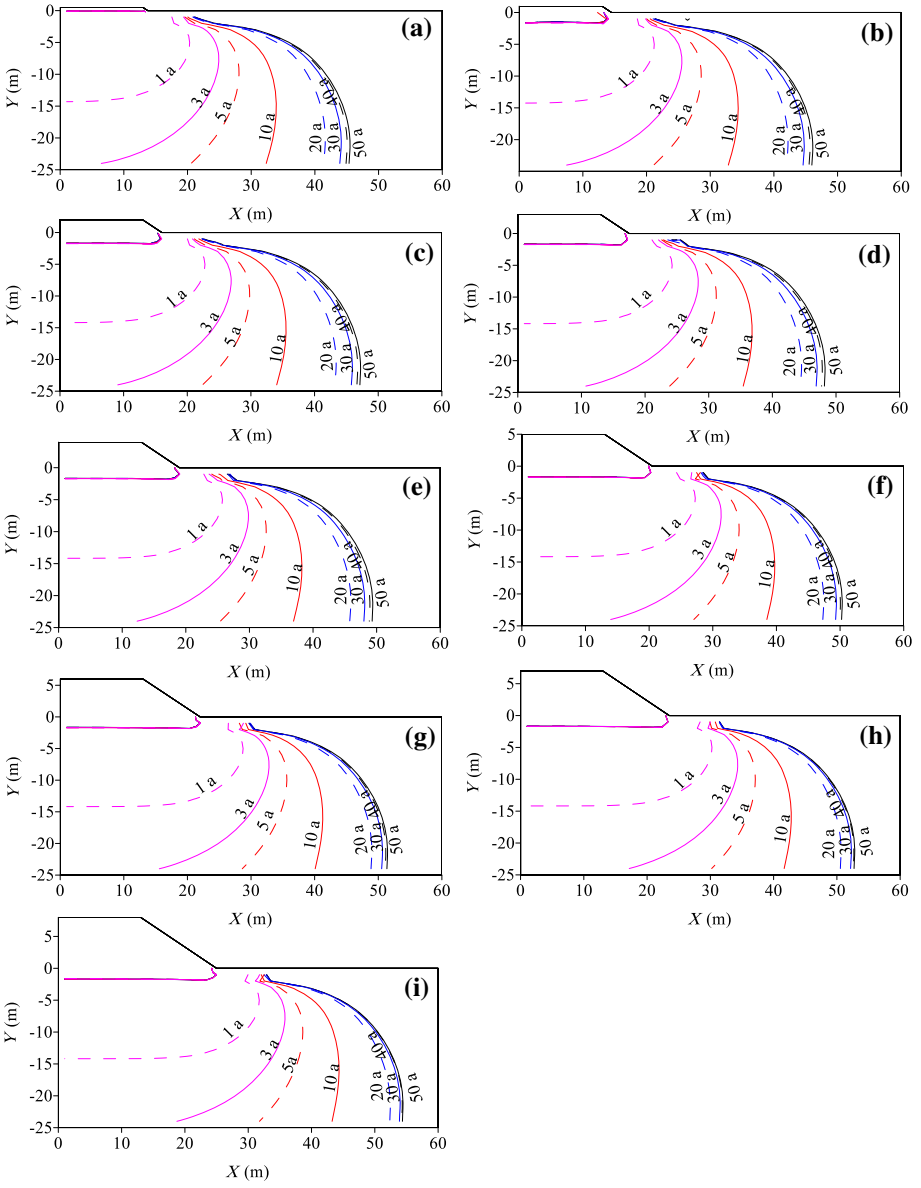

Fig. 17 Isolines for ground temperature change of 0.1 °C under different embankment heights for the full Qinghai-Tibet Expressway. **a** 0.5 m, **b** 1.0 m, **c** 2.0 m, **d** 3.0 m, **e** 4.0 m, **f** 5.0 m, **g** 6.0 m, **h** 7.0 m, and **i** 8.0 m. Isolines are labeled in years (**a**) after construction, and *X* is distance and *Y* is depth

thermal disturbance extent of the full Qinghai-Tibet Expressway is smaller than that of the separated Qinghai-Tibet Expressway with double embankments, it is more difficult to be built in the area with complex topography or with sensitive permafrost underlain in the Qinghai-Tibet Plateau.

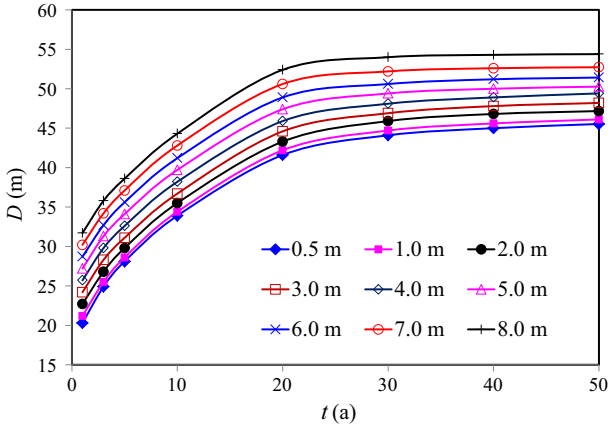

Fig. 18 Temporal changes in the lateral thermal disturbance distance for different embankment heights for the full Qinghai-Tibet Expressway

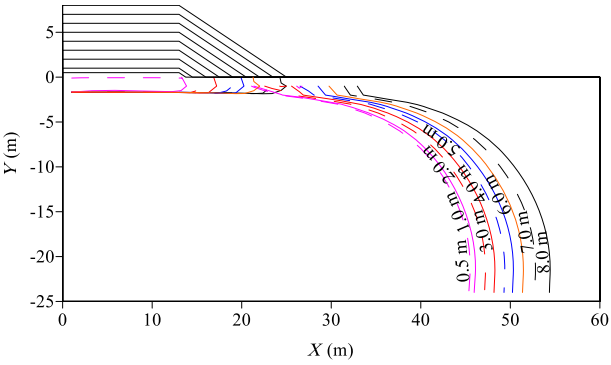

Fig. 19 Thermal disturbance extent for different embankment heights in the 50th year after construction for the full Qinghai-Tibet Expressway

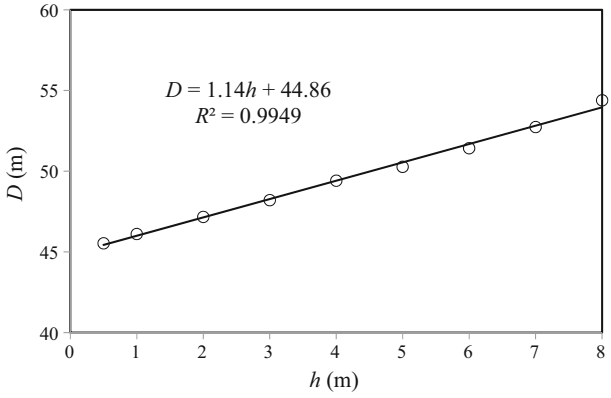

Fig. 20 Relationship between lateral thermal disturbance distance and embankment height for the full Qinghai-Tibet Expressway

In practice, proactive cooling embankment structures can be an effective measure to dissipate or minimize the thermal disturbance. The structures, i.e., crushed-rock embankment, thermosyphon embankment, etc., can have a good cooling effect on the

Table 5 Lateral thermal disturbance distance for different embankment heights for the full Qinghai-Tibet Expressway

Embankment height (m)	Lateral thermal disturbance distance (m)
0.5	45.53
1.0	46.11
2.0	47.17
3.0	48.20
4.0	49.41
5.0	50.27
6.0	51.42
7.0	52.73
8.0	54.39

Table 6 Regression equations between lateral thermal disturbance distance and embankment height for the different embankments

	Regression equation	R^2
Qinghai-Tibet Railway	$D = 3.07\ h + 16.14$	0.9958
Qinghai-Tibet Highway	$D = 2.11\ h + 25.58$	0.9954
Qinghai-Tibet Expressway		
Separated	$D = 1.69\ h + 31.33$	0.9964
Full	$D = 1.14\ h + 44.86$	0.9949

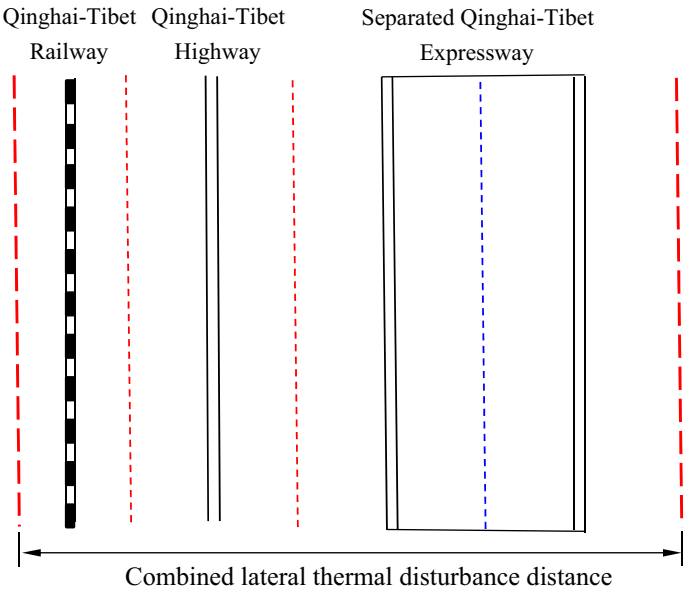

Fig. 21 Schematic of the combined lateral thermal disturbance distance for the Qinghai-Tibet Railway, the Qinghai-Tibet Highway, and the separated Qinghai-Tibet Expressway

subgrades of the Qinghai-Tibet Railway and the Qinghai-Tibet Highway (Yang et al. 2005; Cheng et al. 2008; Wu et al. 2010; Mu et al. 2012; Song et al. 2013; Xi et al. 2014). Some research (Lai et al. 2009b; Gu et al. 2010; Zhang et al. 2010) also shows that composite

embankments combined with different proactive cooling structures can be applied to the planed Qinghai-Tibet Expressway, i.e., crushed-rock interlayer embankment with ventilated duct, embankment with L-shaped thermosyphon, insulation and crushed-rock revetment, etc. Using these embankment structures, the width of the Qinghai-Tibet Engineering Corridor can be reduced or more engineering projects can be accommodated in the engineering corridor.

5 Conclusions

Many structures have been built in the Qinghai-Tibet Engineering Corridor, and there is concern that thermal disturbance of these structures exacerbates degradation of the underlying permafrost. Numerical simulation of the thermal disturbance zones of the three major linear engineering projects in the Qinghai-Tibet corridor, the Qinghai-Tibet Railway, the Qinghai-Tibet Railway, and Qinghai-Tibet Expressway leads to the following conclusions:

1. The lateral extent of thermal distance increases linearly with embankment height for the three embankment types.
2. Under the same embankment heights, the lateral extent of thermal disturbance of the Qinghai-Tibet Railway is smallest because of its relatively narrow and moderate top surface of railway ballast layer, and the full Qinghai-Tibet Expressway is largest because of its wide and high-temperature asphalt top surface.
3. The lateral thermal disturbance extents of the three embankment types is beneficial to quantitatively evaluate the potentially thermal interaction between the current Qinghai-Tibet Railway and Qinghai-Tibet Highway, and to estimate the reasonable scope of the planned Qinghai-Tibet Expressway in the Qinghai-Tibet Engineering Corridor.

In future research it will be important to simulate the lateral extent of thermal disturbance of other engineering structures in the Qinghai-Tibet Engineering Corridor, including tunnels, bridges, and oil pipelines, under current and future climate change scenarios in order to evaluate the potential for additional thermal disturbance. This will allow for a meaningful estimate of the thermal tolerance capacity of the narrow Qinghai-Tibet Engineering Corridor.

Acknowledgments This research was supported by the CAS Action-Plan for West Development (Grant No. KZCX2-XB3-19), the National Natural Science Foundation of China (Grant No. 41471063), the 100-Talent Program of the Chinese Academy of Sciences (Granted to Dr. Mingyi Zhang), the National key Basic Research Program of China (973 Program Grant No. 2012CB026102), the Knowledge Innovation Program of the Chinese Academy of Sciences (Grant No. KZCX2-EW-QN301), and the Youth Innovation Promotion Association CAS.

References

An WD (1990) Interaction among temperature, moisture and stress fields in frozen soil. Lanzhou University Press, Lanzhou

Bonacina C, Comini G, Fasano A, Primicerio M (1973) Numerical solution of phase-change problems. Int J Heat Mass Transf 16:1825–1832

Chen JB, Liu ZY, Jin L (2012) Maximum design height of Qinghai-Tibetan highway embankment. J Xi'an Univ Sci Technol 32(2):198–203
Cheng GD (2002) Interaction between Qinghai-Tibet railway engineering and permafrost and environmental effects. Bull Chin Acad Sci 1:21–25
Cheng GD (2005) A roadbed cooling approach for the construction of Qinghai–Tibet Railway. Cold Reg Sci Technol 42(2):169–176
Cheng GD, Sun ZZ, Niu FJ (2008) Application of the roadbed cooling approach in Qinghai-Tibet railway engineering. Cold Reg Sci Technol 53(3):241–258
Gu W, Yu QH, Qian J, Jin HJ, Zhang JM (2010) Qinghai-Tibet Expressway experimental research. Sci Cold Arid Reg 2(5):396–404
Guo KL, Kong XQ, Chen SN (1999) Computational heat transfer. University of Science and Technology of China Press, Hefei
Jin HJ, Yu QH, Wang SL, Lü LZ (2008) Changes in permafrost environments along the Qinghai-Tibet engineering corridor induced by anthropogenic activities and climate warming. Cold Reg Sci Technol 53:317–333
Kong XY (1999) Advanced mechanics of fluids in porous media. University of Science and Technology of China Press, Hefei
Kong XY, Wu JB (2002) A bifurcation study of non-Darcy free convection in porous media. Acta Mech Sin 34(2):177–185
Lai YM, Zhang LX, Zhang SJ, Mi L (2003) Cooling effect of ripped-stone embankments on Qing-Tibet railway under climatic warming. Chin Sci Bull 48(6):598–604
Lai YM, Zhang MY, Li SY (2009a) Theory and application of cold regions engineering. Science Press, Beijing
Lai YM, Guo HX, Dong YH (2009b) Laboratory investigation on the cooling effect of the embankment with L-shaped thermosyphon and crushed-rock revetment in permafrost regions. Cold Reg Sci Technol 58(3):143–150
Ma W, Niu FJ, Mu YH (2012) Basic research on the major permafrost projects in the Qinghai-Tibet plateau. Adv Earth Sci 11(27):1185–1191
Ministry of Transport of the People's Republic of China (2006) Design specification for highway alignment. China Communications Press, Beijing
Mu YH, Ma W, Wu QB, Sun ZZ, Liu YZ (2012) Cooling processes and effects of crushed rock embankment along the Qinghai-Tibet Railway in permafrost regions. Cold Reg Sci Technol 78:107–114
Nield DA, Bejan A (1992) Convection in porous media. Springer, New York
Niu FJ, Ma W, Wu QB (2011) Thermal stability of roadbeds of the Qinghai-Tibet railway in permafrost regions and the main freezing-thawing hazards. J Earth Sci Environ 33(2):196–206
Peng H, Ma W, Mu YH, Jin L, Yuan K (2015) Degradation characteristics of permafrost under the effect of climate warming and engineering disturbance along the Qinghai-Tibet Highway. Nat Hazards 75:2589–2605
Qin DH, Yao TD, Ding YJ, Ren JW (2014) Glossary of cryosphere science. China Meteorological Press, Beijing
Railway Ministry of the People's Republic of China (2003) Temporary code for engineering construction of railway in permafrost regions of the Qinghai-Tibet Plateau. Beijing, China
Song Y, Jin L, Zhang JZ (2013) In-situ study on cooling characteristics of two-phase closed thermosyphon embankment of Qinghai-Tibet Highway in permafrost regions. Cold Reg Sci Technol 93:12–19
Wang SJ, Huo M, Zou WJ (2004) Subgrade failure of Qinghai-Tibet highway in permafrost area. Highway 5:22–26
Wu QB, Tong CJ (1995) Permafrost change and stability of Qinghai-Tibet highway. J Glaciol Geocryol 17(4):350–355
Wu ZW, Cheng GD, Zhu LN, Liu YZ (1988) Roadbed engineering in permafrost region. Lanzhou University Press, Lanzhou
Wu QB, Shi B, Liu YZ (2003) Interaction study of permafrost and highway along Qinghai-Xizang Highway. Sci China (Ser D) 46(2):97–105
Wu JJ, Ma W, Sun ZZ, Wen Z (2010) In-situ study on cooling effect of the two-phase closed thermosyphon and insulation combinational embankment of the Qinghai-Tibet Railway. Cold Reg Sci Technol 60:234–244
Xi JM, Zhang SL, Chen JB, Jin L, Dong YH (2014) Analysis of the cooling effect of block stone embankment at Wudaoliang section of the Qinghai-Tibet Highway. China J Highw Transp 27(7):17–23
Yang YP, Wei QC, Zhou SH, Zhang LX (2005) Thermosyphon technology and its application in permafrost. Chin J Geotech Eng 27(6):698–706

Zhang MY, Liu DR, Li SY, Zhao AG (2009) Experimental study of the ventilation drag parameters in a railway ballast layer. J Glaciol Geocryol 31(2):372–376
Zhang MY, Lai YM, Dong YH (2010) Three-dimensional nonlinear analysis for the cooling characteristics of crushed-rock interlayer embankment with ventilated duct along the Qinghai-Tibet Expressway in permafrost regions. J Cold Reg Eng 24(4):126–141
Zhao ZN (2002) Heat transfer. Higher Education Press, Beijing
Zhou YW, Guo DX, Qiu GQ, Cheng GD, Li SD (2000) Geocryology in China. Science Press, Beijing
Zhu LN (1988) Study of the adherent layer on different types of ground in permafrost regions on the Qinghai-Xizang Plateau. J Glaciol Geocryol 10(1):8–14